Role of Bud3p in Producing the Axial Budding Pattern of Yeast

John Chant,*‡§ Michelle Mischke,* Elizabeth Mitchell,* Ira Herskowitz,‡ and John R. Pringle§

*Department of Molecular and Cellular Biology, Harvard University, Cambridge, Massachusetts 02138; ‡Department of Biochemistry and Biophysics, University of California, San Francisco, California 94143; and §Department of Biology, University of North Carolina, Chapel Hill, North Carolina 27599-3280

Abstract. Yeast cells can select bud sites in either of two distinct spatial patterns. **a** cells and α cells typically bud in an axial pattern, in which both mother and daughter cells form new buds adjacent to the preceding division site. In contrast, **a**/α cells typically bud in a bipolar pattern, in which new buds can form at either pole of the cell. The *BUD3* gene is specifically required for the axial pattern of budding: mutations of *BUD3* (including a deletion) affect the axial pattern but not the bipolar pattern. The sequence of *BUD3* predicts a product (Bud3p) of 1635 amino acids with no strong or instructive similarities to previously known proteins. However, immunofluorescence localization of Bud3p has revealed that it assembles in an apparent double ring encircling the mother-bud neck shortly after the mitotic spindle forms. The Bud3p structure at the neck persists until cytokinesis, when it splits to yield a single ring of Bud3p marking the division site on each of the two progeny cells. These single rings remain for much of the ensuing unbudded phase and then disassemble. The Bud3p rings are indistinguishable from those of the neck filament-associated proteins (Cdc3p, Cdc10p, Cdc11p, and Cdc12p), except that the latter proteins assemble before bud emergence and remain in place for the duration of the cell cycle. Upon shift of a temperature-sensitive *cdc12* mutant to restrictive temperature, localization of both Bud3p and the neck filament-associated proteins is rapidly lost. In addition, a haploid *cdc11* mutant loses its axial-budding pattern upon shift to restrictive temperature. Taken together, the data suggest that Bud3p and the neck filaments are linked in a cycle in which each controls the position of the other's assembly: Bud3p assembles onto the neck filaments in one cell cycle to mark the site for axial budding (including assembly of the new ring of neck filaments) in the next cell cycle. As the expression and localization of Bud3p are similar in **a**, α, and **a**/α cells, additional regulation must exist such that Bud3p restricts the position of bud formation in **a** and α cells but not in **a**/α cells.

CELL polarization along particular axes and the specific orientation of mitotic spindles and cleavage planes are two recurring themes in the development and functioning of multicellular organisms (Strome, 1993). For example, cell polarization along appropriate axes is central to the interaction of T cells with their targets, the extension of axons by neurons, and the migration of cells crawling on a surface (Singer and Kupfer, 1986). The specific orientation of mitotic spindles and cleavage planes is central to the early embryogenesis of *Caenorhabditis elegans* (Hyman and White, 1987), establishment of sinistral or dextral body plans in snails (Meshcheryakov and Beloussov, 1973; Freeman and Lundelius, 1982), and plant morphogenesis (Gunning, 1982).

Address correspondence to Dr. John Pringle, Department of Biology, CB#3280, University of North Carolina, Chapel Hill, NC 27599-3280. Tel.: (919) 962-2293. Fax: (919) 962-0320 or to Dr. John Chant, Department of Molecular and Cellular Biology, 7 Divinity Avenue, Harvard University, Cambridge, MA 02138. Tel.: (617) 496-9003; Fax: (617) 495-0758.

Similar processes occur during the cell division cycle of budding yeast. Before bud formation, the cell polarizes towards the future bud site (Drubin, 1991; Chant and Pringle, 1991). Selection of the bud site determines the plane of eventual cell division, and the spindle aligns itself along the mother-bud axis so that both mother and daughter cells receive a nucleus. Bud sites can be selected in either of two distinct spatial patterns, termed axial and bipolar (see Chant and Pringle, 1995, and references therein). The choice between these patterns is controlled by the mating-type locus. **a** cells (*MATa*) and α cells (*MAT*α) typically bud in the axial pattern, in which the mother and daughter cells form their new buds directly adjacent to the immediately preceding division site, as marked by the bud scar on the mother cell and the birth scar on the daughter cell. **a**/α cells typically bud in the bipolar pattern, in which the daughter cell usually buds at the pole distal to its birth scar, and the mother cell can bud near either pole of its ellipsoidal shape. Five genes whose products appear dedicated to producing these defined patterns of bud-site selection are known (Bender and Prin-

gle, 1989; Chant and Herskowitz, 1991; Chant et al., 1991). *RSR1/BUD1*, *BUD2*, and *BUD5* are required to produce either pattern: mutations in these genes produce random bud-site selection in **a**, α, and **a**/α cells. In contrast, *BUD3* and *BUD4* appear to be required specifically to produce the axial pattern: mutations in these genes do not affect the bipolar budding of **a**/α cells and cause **a** and α cells also to bud in a bipolar pattern.

After bud-site selection and at least 15 min before the bud emerges, the actin cytoskeleton and cytoplasmic microtubules polarize towards the selected site (Kilmartin and Adams, 1984; Snyder et al., 1991; Ford and Pringle, 1991), and several proteins assemble at that site. This polarization requires the action of several gene products (the so-called "polarity-establishment functions") and is necessary for subsequent targeting of secretion and new cell surface growth to the bud (Drubin, 1991; Chant and Pringle, 1991). The proteins that assemble at the presumptive bud site include several (Spa2p, Cdc42p, and Bem1p) that appear to be involved in polarity establishment (Snyder, 1989; Ziman et al., 1993; Corrado, K., and J. R. Pringle, manuscript submitted for publication) and the neck filament-associated proteins. The latter proteins (the products of genes *CDC3*, *CDC10*, *CDC11*, and *CDC12*) appear to be constituents of the 10-nm filaments that lie just under the plasma membrane in the neck region of budded cells (Byers and Goetsch, 1976; Byers, 1981; Haarer and Pringle, 1987; Kim et al., 1991; Ford and Pringle, 1991; Kim, H., S. Ketcham, B. Haarer and J. R. Pringle, unpublished). Mutations affecting these proteins cause a delocalization of chitin deposition (Adams, 1984), the formation of elongated buds (Adams and Pringle, 1985), a cytokinesis defect (Hartwell, 1971), and a defect in the axial pattern of budding (Flescher et al., 1993; this study).

One plausible model to explain the axial budding pattern is that the site of the preceding division is transiently marked by proteins or other structures laid down at the mother-bud neck in the previous cell cycle (Chant and Herskowitz, 1991; Snyder et al., 1991; Chant and Pringle, 1995). The axial-specific bud-site selection proteins (Bud3p and Bud4p) would be involved in making or recognizing this mark, which would then serve to localize the action of the general bud-site-selection proteins (Rsr1p/Bud1p, Bud2p, and Bud5p), which would in turn communicate with the polarity-establishment proteins to direct their actions to axial sites.

This paper concerns the role of Bud3p in the production of the axial pattern of budding. We report that Bud3p assembles as an apparent double ring in the mother-bud neck before nuclear division and cytokinesis, and it remains localized after division as a single ring on the surface of both mother and daughter cells. It is thus in position to serve as the signal that determines the bud site in the next cell cycle. Furthermore, immunolocalization and genetic observations suggest that the neck filaments or associated proteins act as the template for Bud3p assembly.

Materials and Methods

Strains, Growth Conditions, and Genetic Methods

Yeast strains and plasmids are described in Table I. Standard yeast genetic procedures and media were used as described elsewhere (Rose et al., 1990). Except where noted, yeast strains were grown at 30°C in YM-P rich medium (Lillie and Pringle, 1980). For temperature shifts of *cdc* mutants, cells were grown overnight at 23°C to ~2 × 10^7 cells/ml and then diluted fivefold into medium that had been prewarmed to 37°C. Cells were arrested with nocodazole as described by Jacobs et al. (1988) using 20 μg/ml nocodazole (Sigma Chem. Co., St. Louis, MO). Cells were arrested with 0.2 M hydroxyurea (Sigma) as described by Slater (1973).

DNA and RNA Manipulations

Except as noted, standard procedures were used for DNA and RNA manipulations including Southern and Northern blot analyses (Sambrook et al., 1989). *E. coli* strain DH5α (Sambrook et al., 1989) was used for most cloning procedures. *E. coli* strains HB101 (Sambrook et al., 1989) and BMH71-18 (Rüther and Müller-Hill, 1983) were used for expressing *trpE* and *lacZ* fusion constructs, respectively. Yeast transformations were performed by the lithium acetate method (Ito et al., 1983). For DNA sequencing, fragments were subcloned into M13mp18 and M13mp19 (Messing, 1983), and single-stranded DNA was sequenced by the dideoxy chain termination method (Sanger et al., 1977). For certain regions, oligonucleotides were synthesized as primers for sequencing. Sequence obtained from one strand was compared to the published sequence of this region (Oliver et al., 1992). Where differences were found between our sequence and the published sequence that changed the length of the *BUD3* open reading frame, oligonucleotide primers were used to confirm our sequence on the opposite strand.

Disruption and Deletion of BUD3

The *BUD3* disruption was constructed by ligating a blunt-ended EcoRI fragment containing *TRP1* (from pUC18::*TRP1*, obtained from B. Patterson) into a blunt-ended BglII site of *BUD3* in plF8 (Fig. 1, pBUD3I). The resulting plasmid was linearized by cleavage with EcoRI and transformed into the diploid strain JC600.

Both the partial and complete *BUD3* deletions were constructed by a combination of polymerase chain reaction and standard procedures (Vallette et al., 1989). *bud3Δ#1* (partial gene deletion): with pl3 (Fig. 1) as template, *BUD3* 5′-flanking sequences were amplified using VENT polymerase (New England Biolabs, Beverly, MA) under the recommended conditions with primers 5′-1 (GGATCCTGTATTATATCCAGT) and 5′-2 (ATCGATGGATCCACTAGTTGGTGAGGTGTAAATATACTC). The amplified DNA (an ~600-bp fragment) was digested with BamHI (sites from the primers) and ligated into the BamHI site of pUC119 (Messing, 1983), thereby creating pUC119-5′. Similarly, sequences in the 3′ half of the *BUD3* open reading frame were amplified using primers 3′-1 (ACTAGTGGATCCATCGATTAACATTTCCAATTTTGCAGA) and 3′-2 (CATTTGATACGCCCTTTTCTT). The amplified DNA (an ~400-bp fragment) was cut with BamHI (site from primer 3′-1) and XhoI (site immediately 3′ of primer 3′-2) and ligated into pUC119 via its BamHI and XhoI sites, thereby creating pUC119-3′. The BamHI fragment of plasmid pUC119-5′ was ligated into plasmid pUC119-3′ that had been linearized with BamHI, thereby joining the *BUD3* 5′- and 3′-flanking sequences in pUC119. The ligation products were screened by restriction-site analysis for the orientation of the 5′-flanking sequences relative to the 3′-flanking sequences, and a clone with the orientation corresponding to that in the chromosome was identified (pUC119-5′,3′). A SpeI-ClaI fragment containing *TRP1* was isolated from plasmid pKS-TRP-B (provided by S. Lillie) and cloned into SpeI/ClaI-digested pUC119-5′,3′ (SpeI site just 3′ of primer 5′-2; ClaI site from primer 3′-1), thereby creating a construct in which *TRP1* is flanked by sequences 5′ of *BUD3* and in the 3′ half of the gene (plasmid pBUD3Δ#1, Fig. 1). In pBUD3Δ#1, the NH_2-terminal 994 codons of the *BUD3* open reading frame plus 100 additional base pairs from the *BUD3* 5′-flanking region were removed. Plasmid pBUD3Δ#1 was linearized by cleavage with SphI and PvuII (both sites in pUC119) and used to transform strain 1237-13C. Seven Trp^+ transformants were isolated and scored for budding pattern. Three transformants displayed bipolar budding patterns, suggesting that *BUD3* had been deleted. Gene deletion was confirmed in these three strains by Southern blot hybridization (data not shown). Southern blot analyses of the remaining transformants, which displayed axial budding, revealed a wild-type pattern of bands from the *BUD3* locus, confirming that gene replacement had not occurred.

bud3Δ#2 (complete gene deletion): With pl3 as template, *BUD3* 5′-flanking sequences were amplified as described above, using primers BUD3-G (CCGGATCCTGTATTATATCCAG) and BUD3-H (CGGAATTCAAGCTTCTCCATTGGTGAGGTG). The amplified DNA (an ~600-bp fragment) was digested with BamHI and EcoRI (sites from the primers) and ligated via the corresponding sites into a derivative of pUC119 lacking the HindIII site to yield pUC119-GH. Similarly, *BUD3* 3′-flanking sequences

Table I. Yeast Strains and Plasmids Used in This Study

Strain	Relevant genotype	Source
1784	*MATα his4 leu2 trp1 ura3*	Tatchell et al., 1981
1237-13C	*MATα HMRα HMLα his4 trp1 ura3*	Chant and Herskowitz, 1991
1241-2D	*MATa HMRα HMLα leu2 trp1 ura3*	Chant and Herskowitz, 1991
29	*matal⁻ his4 trp1 ura3*	Chant and Herskowitz, 1991
52	*MATa/MATα his4/his4 trp1/trp1 ura3/ura3*	Chant and Herskowitz, 1991
103	*matal⁻ his4 trp1 ura3 bud3-1*	Chant and Herskowitz, 1991
128	*MATα HMRα HMLα his4 trp1 ura3 bud3-1*	Chant and Herskowitz, 1991
C276	*MATa/MATα* (prototroph)	Wilkinson and Pringle, 1974
C276-4A	*MATa* (prototroph)	Wilkinson and Pringle, 1974
CP1AB-1BB	*MATα/MATα* (prototroph)	Paquin and Adams, 1982
486	*MATα HMRα HMLα his4 trp1 ura3 bud3::TRP1*	This study*
489	*MATa/MATα HIS4/his4 URA3/ura3 bud3::TRP1/bud3::TRP1*	This study‡
490	*MATa/MATα HIS4/his4 URA3/ura3 BUD3/BUD3*	This study‡
493	*MATa/MATα HIS4/his4 ura3/ura3 bud3::TRP1/bud3::TRP1*	This study‡
JC600	*MATa/MATα HIS4/his4 LEU2/leu2 trp1/trp1 ura3/ura3*	1237-13C X 1241-2D
JC601	*MATa/MATα HIS4/his4 LEU2/leu2 trp1/trp1 ura3/ura3 bud3::TRP1/BUD3*	1241-2D X 486
JC602	*MATa/MATα HIS4/his4 LEU2/leu2 trp1/trp1 ura3/ura3 bud3::URA3/BUD3*	Transformant of JC601§
MM 5.1	*MATa his4 LEU2 trp1 ura3 bud3::URA3*	Segregant from JC602
MM 5.2	*MATa HIS4 leu2 trp1 ura3*	Segregant from JC602
MM 5.3	*MATα HIS4 leu2 trp1 ura3*	Segregant from JC602
MM 5.4	*MATα his4 LEU2 trp1 ura3 bud3::URA3*	Segregant from JC602
MMd1	*MATa/MATα his4/his4 LEU2/LEU2 trp1/trp1 ura3/ura3 bud3::URA3/bud3::URA3*	MM5.1 X MM5.4
MMd2	*MATα/matal⁻ his4/his4 trp1/trp1 ura3/ura3 bud3::URA3/bud3-1*	MM5.4 X 103
MMd3	*MATα/matal⁻ his4/his4 trp1/trp1 ura3/ura3 bud3::URA3/BUD3*	MM5.4 X 29
JPTA1493-HO1	*MATa/MATα cdc12-6/cdc12-6* (prototroph)	Adams and Pringle, 1984
T515A	*MATa cdc11-6 met1*	H. Fares

Plasmid	Description	Source
YCp50	*URA3*-containing, centromere-containing plasmid (low copy number)	Rose et al., 1987
p35-1	Original isolate of *BUD3* plus *LEU2* in YCp50	This study‖
plF8, plB2, pl3	Subclones of *BUD3* in YCp50	This study‖
pBUD3I	plF8 with the *BUD3* coding region disrupted by insertion of *TRP1*	This study‖
pBUD3Δ#1	pUC119 carrying *BUD3* with NH_2-terminal coding region deleted and replaced by *TRP1*	This study‖
pBUD3Δ#2	pUC119 carrying *BUD3* region with *BUD3* open reading frame deleted and replaced by *URA3*	This study‖

* *BUD3* gene deletion strain (see text and Fig. 1, pBUD3Δ#1).
‡ Diploids constructed by mating segregants from the third backcross of 486 to C276-4A.
§ See text and Fig. 1 (pBUD3Δ#2).
‖ See Fig. 1 and associated text.

were amplified using primers BUD3-I (CGGAATTCCGAAGCTTACTGAAATTTTATTGAGTG) and BUD3-J (CGCGAATTCACAGATCTCTTATGCTAGACG). The amplified DNA (an ~900-bp fragment) was digested with EcoRI (sites from the primers) and ligated into pUC119 (lacking the HindIII site) via its EcoRI site to yield pUC119-IJ. pUC119-GH was linearized with EcoRI and HindIII (site from primer BUD3-H), and the *BUD3* 3'EcoRI-HindIII fragment liberated from pUC119-IJ (HindIII site from primer BUD3-I) was ligated into the compatible ends of the linearized pUC119-GH. The resulting plasmid, pUC119-GHIJ, carrying the *BUD3* 5'- and 3'-flanking regions in their natural order, was linearized with HindIII, and a *URA3* HindIII fragment from YIp-URA (provided by S. Lillie) was ligated into this site to produce the complete *BUD3*-deletion construct (pBUD3Δ#2, Fig. 1), in which all of the *BUD3* coding sequence was precisely replaced with *URA3*. Plasmid pBUD3Δ#2 was linearized by cleavage with BamHI and EcoRI and used to transform strain JC601. Ura^+ Trp^- transformants were isolated and tetrads were dissected. A 2:2 segregation of budding patterns was observed, with Ura^+ linked to bipolar budding in all 8 tetrads examined, indicating that *BUD3* had been deleted. Gene deletion was confirmed by Southern blot analyses of several tetrads (Fig. 2 *A*). Bipolar budding segregants exhibited a pattern of bands indicating the replacement of *BUD3* by *URA3*, whereas axially budding segregants exhibited a wild-type pattern of bands from the *BUD3* locus.

Analysis of Growth, Budding Pattern, and Mating

The growth of *BUD3*-deletion strains was assessed by comparing the sizes of colonies produced to those of wild-type strains on rich and minimal medium at 30°C and 23°C. Budding patterns were scored either by observing cells grown on agar (Chant and Herskowitz, 1991) or by staining bud scars with Calcofluor and observing by fluorescence microscopy (Pringle, 1991). The mating of *BUD3*-deletion strains with wild type was scored by the standard mating patch test (Sprague, 1991). Mating of α *BUD3*-deletion by a *BUD3*-deletion strains was scored by counting zygotes in mating mixtures 3 h after mixing.

Production of Antibodies to Bud3p

BUD3 was fused to *lacZ* and to *trpE* by ligating the BglII-ClaI fragment of *BUD3* (Fig. 1) into pUR278 (Rüther and Müller-Hill, 1983) and pATH2

(Koerner et al., 1991), respectively, using the BamHI and ClaI sites in each vector. The *lacZ-BUD3* and *trpE-BUD3* fusions were induced with IPTG and indole acrylic acid, respectively (Kim et al., 1991; Snyder, 1989). Each fusion protein was isolated as an insoluble fraction (Kleid et al., 1981), and two rabbits per protein were injected subcutaneously with 500 μg of protein plus Freund's complete adjuvant. Each rabbit was boosted four to five times at 30-d intervals by injection of 250 μg of protein with Freund's incomplete adjuvant. Responses were monitored by Western blot analysis (Sambrook et al., 1989) of proteins from the appropriate *E. coli* strains. The best responses were observed after the fourth and fifth boosts in one of the rabbits injected with the β-galactosidase-Bud3p fusion protein. Before use in immunofluorescence experiments, the antibodies from this rabbit were double affinity purified using the nitrocellulose-strip method (Pringle et al., 1991), first on a strip containing β-galactosidase-Bud3p, and then on a strip containing anthranilate synthase-Bud3p. The strips of nitrocellulose were eluted twice with 4 M $MgCl_2$ plus 0.1% bovine serum albumin (BSA), and then once with 2.5 M glycine, pH 2.5, plus 0.1% BSA (immediately neutralized with 100 mM Tris base after elution). The eluted fractions were washed several times with PBS in a Centricon 30 concentrator, concentrated, and then combined. The double affinity-purified serum was then preadsorbed two to four times against spheroplasts and whole cells prepared from the *bud3* deletion strain 489; ~10^8 cells were used per cycle of adsorption. Double affinity purified and preadsorbed serum was used undiluted in immunofluorescence procedures.

Immunofluorescence

Indirect immunofluorescence was performed as described by Pringle et al. (1991). A rat monoclonal antibody (YOL1/34) was used to visualize microtubule structures (Kilmartin and Adams, 1984; Adams and Pringle, 1984), and an affinity-purified rabbit polyclonal antibody was used to visualize the neck filament-associated protein Cdc3p (Kim et al., 1991). The secondary antibodies used were FITC-conjugated goat anti-rabbit IgG and rhodamine-conjugated goat anti-rat IgG (Jackson Immunoresearch Laboratories, West Grove, PA). To visualize nuclei, bis-benzamide (Sigma) was added after the seventh rinse after incubation with the secondary antibody, and incubation was continued for 5 min before the remaining three rinses. Rhodamine phalloidin (Molecular Probes, Eugene, OR) was used to visualize actin as described by Adams and Pringle (1991). Fluorescence microscopy was performed using a Nikon Microphot SA microscope with a 63× Plan-apo objective.

Results

Isolation and Sequence Analysis of BUD3

Linkage analysis indicated that *BUD3* is ~4 cM from *LEU2* (Chant and Herskowitz, 1991), suggesting that it might be possible to clone *BUD3* by screening *LEU2*-containing plasmids from an appropriate library. Accordingly, strain 1784 (*leu2*) was transformed with a library of Sau3A partial-digestion fragments in the *URA3*-based, low copy number vector YCp50 (Rose et al., 1987), and 14 Leu$^+$ clones were isolated. Plasmids were recovered into *E. coli* and then transformed into strain 128 to test for complementation of the *bud3* mutation. Two of the 14 plasmids restored axial budding, as judged by the observation of transformants budding on agar, indicating that these plasmids probably contained *BUD3*. One of these plasmids (p35-1) was analyzed further (Fig. 1 *A*).

The *bud3*-complementing activity was localized to a 3.4-kb BamHI-EcoRI segment by subcloning (Fig. 1 *B*). This localization was confirmed by insertion of *TRP1* at the BglII site within that segment (Fig. 1 *C*; see Materials and Methods). Linear DNA carrying the *TRP1* insertion was transformed into the diploid strain JC600 (*BUD3/BUD3 LEU2/leu2 trp1/trp1*), a stable Trp$^+$ transformant was isolated, and tetrads were dissected. In ten tetrads scored, bipolar budding cosegregated with Trp$^+$ Leu$^+$, while axial budding cosegregated with Trp$^-$ Leu$^-$, indicating that the copy of *BUD3* in the chromosome carrying *LEU2* had been disrupted. Thus, *BUD3* overlaps the indicated BglII site (Fig. 1).

Fragments derived from subclone p13 (Fig. 1 *B*) were used to obtain ~1 kb of continuous sequence surrounding the BglII site internal to *BUD3*. Comparison of this sequence

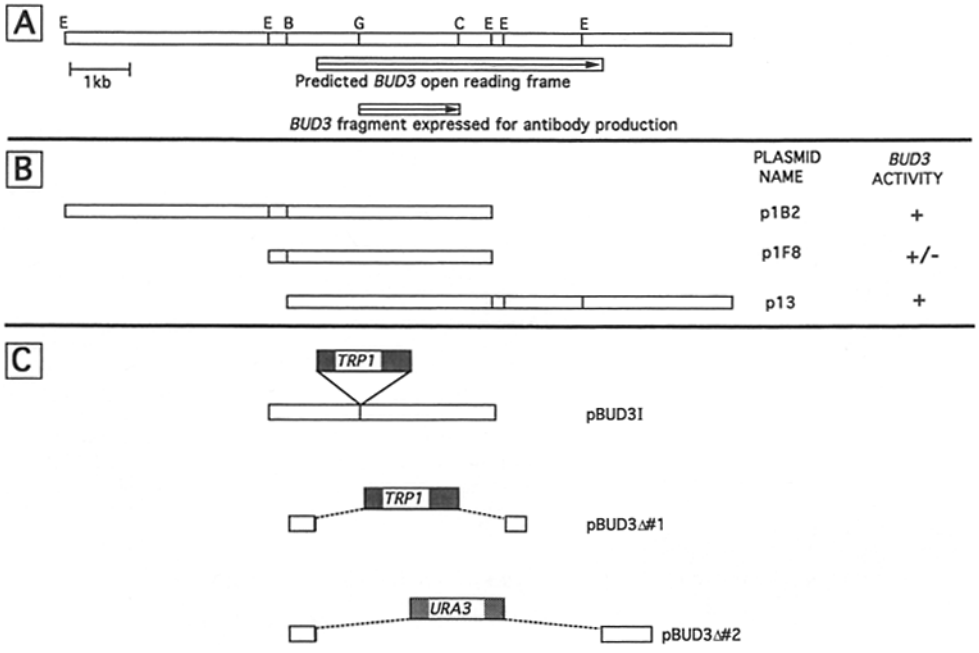

Figure 1. Physical map, subcloning, and deletion of *BUD3*. (*A*) Restriction map of the *BUD3* region. The original isolate, plasmid p35-1, contained additional flanking sequences to the left of those depicted here. The *BUD3* open reading frame inferred from the DNA sequence is indicated, as is the fragment fused to *trpE* and *lacZ* to generate fusion proteins used for antibody production (see text). Restriction sites: *C*, ClaI; *B*, BamHI; *E*, EcoRI; *G*, BglII; *H*, HindIII. There are other ClaI and BglII sites in addition to those shown. (*B*) Subclones of *BUD3* and their ability to restore axial budding to an α *bud3* strain (strain 128) when introduced on the low copy number plasmid YCp50. (*C*) Disruption and deletion constructs of *BUD3* (see text).

to sequences determined in S. Oliver's laboratory as part of the consortium effort to sequence all of chromosome III (Oliver et al., 1992) allowed assignment of *BUD3* to open reading frame YCL14W, predicted to encode a protein of 1004 amino acids (Oliver et al., 1992). However, the presence of long open reading frames overlapping and downstream from the predicted termination of YCL14W led us to reexamine the sequence in this region for possible frameshifts that might have caused a misreading of the end of the *BUD3* open reading frame. Indeed, resequencing of this region indicated that the predicted open reading frame continues for a considerable distance and should encode a protein of 1635 amino acids (Fig. 3). The observation that a partial fragment of the *BUD3* open reading frame restored axial budding to the original *bud3-1* mutant (Fig. 2 *B*) may indicate either that the COOH terminus of Bud3p is dispensable for function or that only partial function is required to complement the original *bud3-1* mutation, which may not be a null. (The *BUD3* fragment does partially restore axial budding to a *BUD3*-deletion strain, described below, supporting the first interpretation). No other ATG-initiated open reading frame of greater than 50 codons was found in the region. The revised sequence, which includes several differences from that reported previously, has been deposited in GenBank (U17580). Comparison of the predicted Bud3p sequence with the available databases has to date revealed no strong or instructive similarities.

```
   1 MEKDLSSLYS EKKDKENDET LFNIKLSKSV VETTPLNGHS LFDDDKSLSD WTDNVFTQSV 60
  61 FYHGSDDLIW GKFFVCVYKS PNSNKLNAII FDKLGTSCFE SVDISSNSQY YPAIENLSPS 120
 121 DQESNVKKCI AVILLQRYPL LSPSDLSQIL SNKSENCDYD PPYAGDLASS CQLITAVPPE 180
 181 DLGKRFFTSG LLQNRFVSST LLDVIYENNE STIELNNRLV FHLGEQLEQL FNPVTEYSPE 240
 241 QTEYGYKAPE DELPTESDDD LVKAICNELL QLQTNFTFNL VEFLPKFLIA LRVRVLNEEI 300
 301 NGLSTTKLNR LFPPTIDEVT RINCIFLDSL KTAIPYGSLE VLKACSITIP YFYKAYTRHE 360
 361 AATKNFSKDI KLFIRHFSNV IPEREVYTEM KIESIIKGPQ EKLLKLNLII ERLWKSKKWR 420
 421 PKNQEMAKKC YNNIIDVIDS FGKLDSPLHS YSTRVFTPSG KILTELAKCW PVELQYKWLK 480
 481 RRVVGVYDVV DLNDENKRNL LVIFSDYVVF INILEAESYY TSDGSNRPLI SDILMNSLIN 540
 541 EVPLPSKIPK LKVERHCYID EVLVSILDKS TLRFDRLKGK DSFSMVCKLS SAFISSSSVA 600
 601 DLITKARILE KDTAFHLFKA SRSHFTLYST AHELCAYDSE KIKSKFALFL NIPPSKEILE 660
 661 VNNLHLAFFA RFCSNDGRDN IVILDVLTKH DDKHIEVTSD NIVFTIINQL AIEIPICFSS 720
 721 LNSSMAKDLL CVNENLIKNL EHQLEEVKHP STDEHRAVNS KLSGASDFDA THEKKRSYGT 780
 781 ITTFRSYTSD LKDSPSGDNS NVTKETKEIL PVKPTKKSSK KPREIQKKTK TNASKAEHIE 840
 841 KKKPNKGKGF FGVLKNVFGS KSKSKPSPVQ RVPKKISQRH PKSPVKKPMT SEKKSSPKRA 900
 901 VVSSPKIKKK STSFSTKESQ TAKSSLRAVE FKSDDLIGKP PDVGNGAHPQ ENTRISSVVR 960
 961 DTKYVSYNPS QPVTENTSNE KNVEPKADQS TKQDNISNFA DVEVSASSYP EKLDAETDDQ 1020
1021 IIGKATNSSS VHGNKELPDL AEVTTANRVS TTSAGDQRID TQSEFLRAAD VENLSDDDEH 1080
1081 RQNESRVFND DLFGDFIPKH YRNKQENINS SSNLFPEGKV PQEKGVSNEN TNISLKTNED 1140
1141 ASTLTQKLSP QASKVLTENS NELKDTNNEG KDAKDIKLGD DYSDKETAKE ITKPKNFVEG 1200
1201 ITERKEIFPT IPRLAPPASK INFQRSPSYI ELFQGMRVVL DKHDAHYNWK RLASQVSLSE 1260
1261 GLKVNTEEDA AIINKSQDDA KAERMTQISE VIEYEMQQPI PTYLPKAHLD DSGIEKSDDK 1320
1321 FFEIEEELKE ELKGSKTGNE DVGNNNPSNS IPKIEKPPAF KVIRTSPVRI IGRTFEDTRK 1380
1381 YENGSPSDIS FTYDTHNNDE PDKRIMELKF PSQDEIPDDR FYTPAEEPTA EFPVEELPNT 1440
1441 PRSINVTTSN NKSTDDKLSS GNIDQKPTEL LDDLEFSSFN IAFGNTSMST DNMKISSDLS 1500
1501 SNKTVLGNAQ KVQESPSGPL IYVLPQVSTK HEKEGFLRKK QKDEPIWVSP SKIDFADLSR 1560
1561 RTKALTPERN TVPLKNNDSR KYKYTGEGSI GNMTNMLLTK DASYAYLKDF VALSDDEDED 1620
1621 GKQNCAVGGP EKLKFY                                             1636
```

Figure 3. Predicted sequence of Bud3p.

Characterization of a BUD3*-Deletion Strain*

The availability of the sequence facilitated construction of a precise deletion of the predicted *BUD3* coding region (Fig. 1 *C*; see Materials and Methods). Haploid strains (MM5.1, MM5.4) carrying this *bud3::URA3* deletion displayed bipolar budding patterns similar to those of wild-type **a**/α cells, just as observed for the original *bud3-1* mutant (Fig. 2 *B*; cf. Chant and Herskowitz, 1991). The deletion was shown to be recessive by constructing the *MAT* α/*mata1*$^-$ *bud3::URA3/BUD3* strain MMd3 (Table I); this strain, which is phenotypically α, displayed normal axial budding. In contrast, the *MAT* α/*mata1*$^-$ *bud3::URA3/bud3-1* strain MMd2 displayed bipolar budding (data not shown). This noncomplementation result confirms that the deletion affects *BUD3*. Interestingly, the other two disrupted alleles of *BUD3* that were constructed, the *TRP1* insertion and the *TRP1* partial deletion, both exhibited dominant-negative phenotypes relative to wild-type *BUD3* (i.e., strains comparable to MMd3 displayed bipolar budding). These mutants probably produce partial Bud3p proteins that interfere with wild-type Bud3p function.

a/α *bud3::URA3/bud3::URA3* strains exhibited normal bipolar budding patterns (Fig. 2 *B*), supporting the previous conclusion (Chant and Herskowitz, 1991) that *BUD3* is dispensable for the bipolar pattern. Moreover, examination of *BUD3*-deletion strains revealed no other abnormal phenotypes. Haploid and diploid *BUD3*-deletion strains grew at rates indistinguishable from those of comparable wild-type strains. Both mating ability (both in *bud3* by wild type and *bud3* by *bud3* crosses; see Materials and Methods) and cell

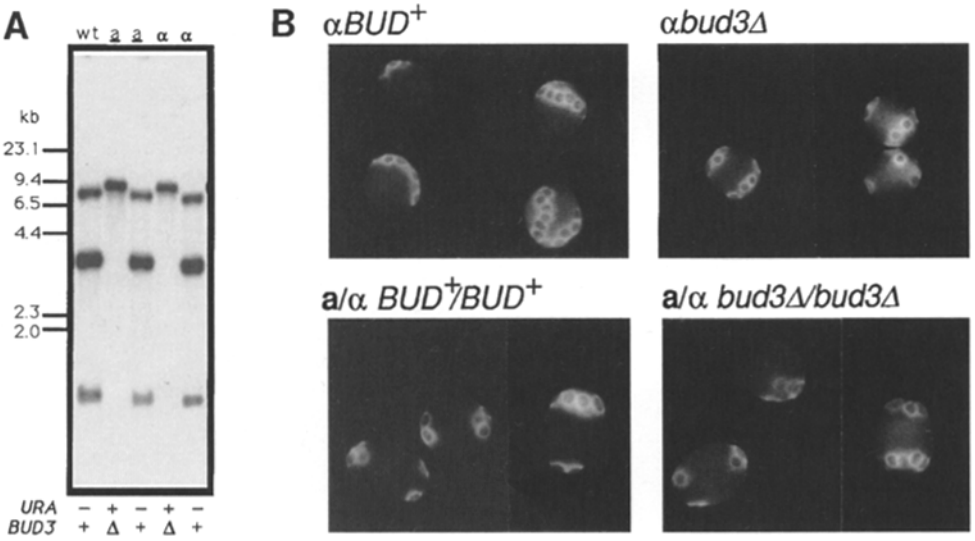

Figure 2. Analysis of wild-type and *BUD3*-deletion strains. (*A*) Southern blot confirming the deletion of *BUD3*. Genomic DNAs from the wild-type strain 1241-2D and the four segregants from one tetrad from strain JC602 were digested with EcoRI and probed with the entire insert from plasmid pl3. (*B*) Bud scar patterns of wild-type and mutant yeast cells of the genotypes indicated. The following strains are illustrated: α *BUD3*$^+$ (strain 1237-13C), α *bud3::URA3* (strain MM5.4), **a**/α *BUD3*$^+$/*BUD3*$^+$ (strain 490), and **a**/α *bud3::URA3*/*bud3::URA3* (strain MMd1).

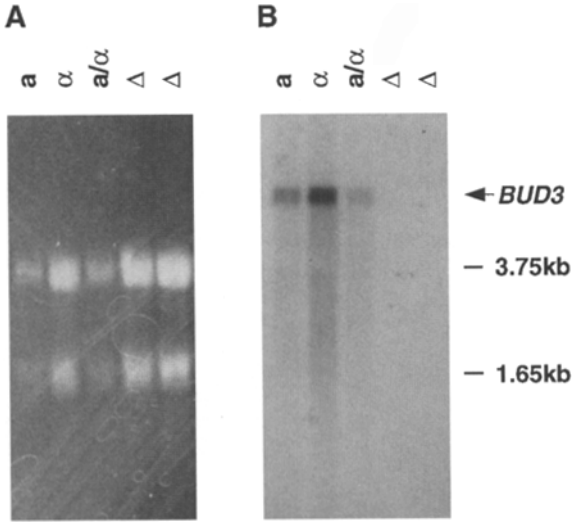

Figure 4. Analysis of *BUD3* expression. (*A*) Ethidium bromide-stained gel to show relative amounts of RNA loaded. The 3.75-kb and 1.65-kb ribosomal RNAs are visualized. (*B*) Detection of *BUD3* transcripts by Northern blot analysis using the 3.7-kb EcoRI–EcoRI fragment as probe. Expression was determined in **a**, α, **a**/α, and *BUD3*-deletion strains (strains 1241-2D, 1237-13C, 52, MM 5.1, and MM5.4, respectively).

morphology appeared identical to those of wild-type strains (data not shown). Thus, deletion of *BUD3* produces no readily detectable phenotypes other than the alteration of budding pattern, as is also the case for deletion of *RSR1/BUD1* (Bender and Pringle, 1989), *BUD2* (Park et al., 1993), *BUD4* (Sanders, S., and I. Herskowitz, unpublished results), and *BUD5* (Chant et al., 1991).

Expression of BUD3 *in a, α, and a/α Cells*

A plausible model for the control of budding pattern by cell type is that expression of one or more genes involved in bud-site selection is regulated by the mating-type locus (*MAT*). For example, a gene (such as *BUD3*) that is necessary specifically for the axial pattern might be repressed in **a**/α cells by the repressor **a**l-α2 that is present only in such cells (Chant and Herskowitz, 1991). To explore this possibility, the expression of *BUD3* in **a**, α, and **a**/α cells was tested by Northern blot analysis. *BUD3* mRNA was detected in all cell types at similar levels. *BUD3* mRNA was absent from the *bud3::URA3* strain (Fig. 4).

Intracellular Localization of Bud3p

To localize Bud3p, immunofluorescence was performed using Bud3p-specific antibodies (see Materials and Methods). In both α/α (axial budding) and **a**/α (bipolar budding) strains, several patterns of staining were observed (Fig. 5, *A* and *B*). Cells with large buds (equal to or greater than half the length of the mother cell) uniformly displayed an apparent double ring of Bud3p encircling the mother-bud neck. In addition, some, but not all, unbudded cells exhibited a single ring of Bud3p at the cell surface. In contrast, cells with small buds displayed no localized staining of Bud3p. The apparent splitting of the Bud3p double rings in cells undergoing division (Fig. 5, *C–E*) suggests strongly that the single rings of Bud3p seen in unbudded cells represent persistence in both mother and daughter cells of the structures assembled at the

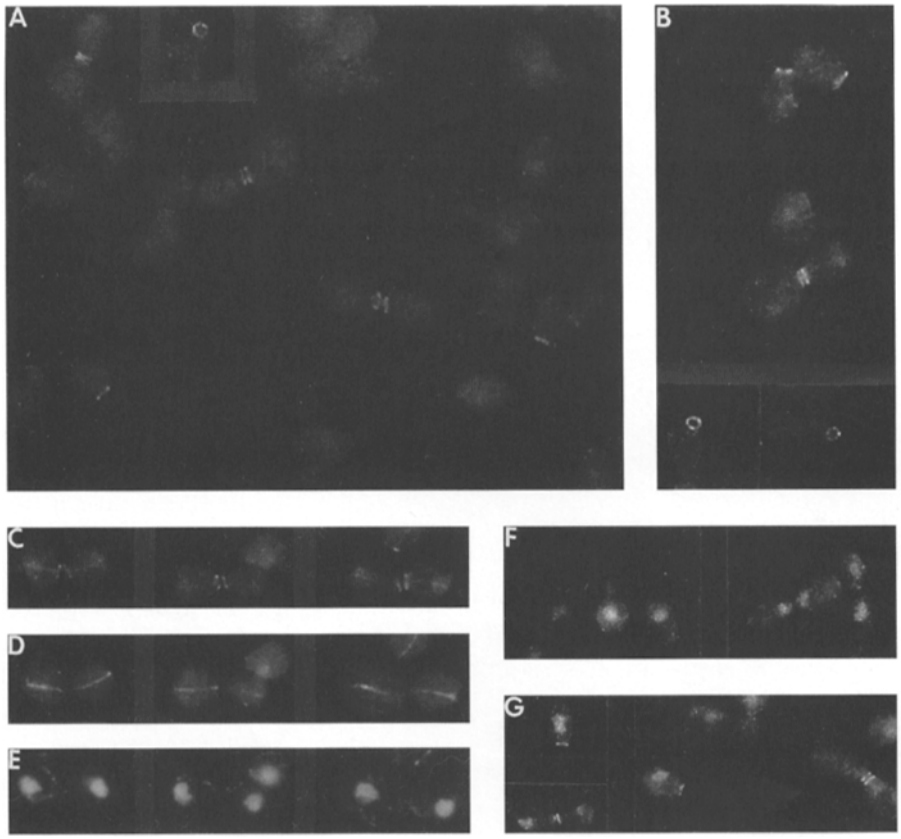

Figure 5. Immunofluorescence localization of Bud3p in vegetatively growing cells. (*A* and *C*) Bud3p localization in the wild-type α/α strain CP1AB-1BB. (An α/α diploid strain was used because of its larger cell size as compared to haploid α strains.) *C* shows cells undergoing cytokinesis. (*B*) Bud3p localization in the wild-type **a**/α strain C276. (*D* and *E*) Antitubulin immunofluorescence (*D*) and DNA staining (*E*) of the same cells as shown in *C*. (*F*) Lack of Bud3p staining in *BUD3*-deletion strain 489; the nuclear staining is weak background staining sometimes observed in both wild-type and deletion strains. (*G*) Bud3p localization in *BUD3*-deletion strain 493 transformed with a low copy number *BUD3* plasmid (pl3).

mother-bud neck during the previous cell cycle (see also below). If so, then the unbudded cells without rings of Bud3p must be cells that are later in the unbudded phase.

The specificity of the Bud3p staining was confirmed by demonstrating that it was *BUD3* dependent. No rings of staining were detected in cells homozygous for the partial *bud3*Δ#1 deletion in several independent experiments (Fig. 5, *F*; note that the region of *BUD3* expressed for antibody production was deleted by the *bud3*Δ#1 deletion). Furthermore, the staining could be restored to this deletion strain by transforming with a low copy number *BUD3* plasmid (Fig. 5 *G*), but not by transforming with vector alone (data not shown; cells were indistinguishable from those shown in Fig. 5 *F*).

To correlate the timing of Bud3p assembly at the neck with events in the nuclear cycle, Bud3p, tubulin, and DNA were stained in triple-labeling experiments (Fig. 6, *A–C*). The vast majority of cells exhibiting prominent double rings of Bud3p also had elongated spindles, indicating that nuclear division was in progress (Fig. 6, *A–C*, cells *5* and *6*). However, some cells with short spindles also exhibited faint Bud3p staining (Fig. 6, *A–C*, cell *4*). The Bud3p signals in these cells were consistently weaker than those in cells with elongated spindles, suggesting that assembly of Bud3p begins in cells with short spindles (a prolonged stage in the yeast cell cycle: Byers and Goetsch, 1975) and continues as the nuclear cycle proceeds.

This interpretation was corroborated and extended by experiments using the cell cycle inhibitors hydroxyurea (which blocks the completion of DNA synthesis and thus causes cells to arrest with a large bud and a single nucleus with a short spindle [Slater, 1973; Weinert and Hartwell, 1993]) and nocodazole (which destabilizes microtubules and thus causes cells to arrest with large buds, replicated DNA, and

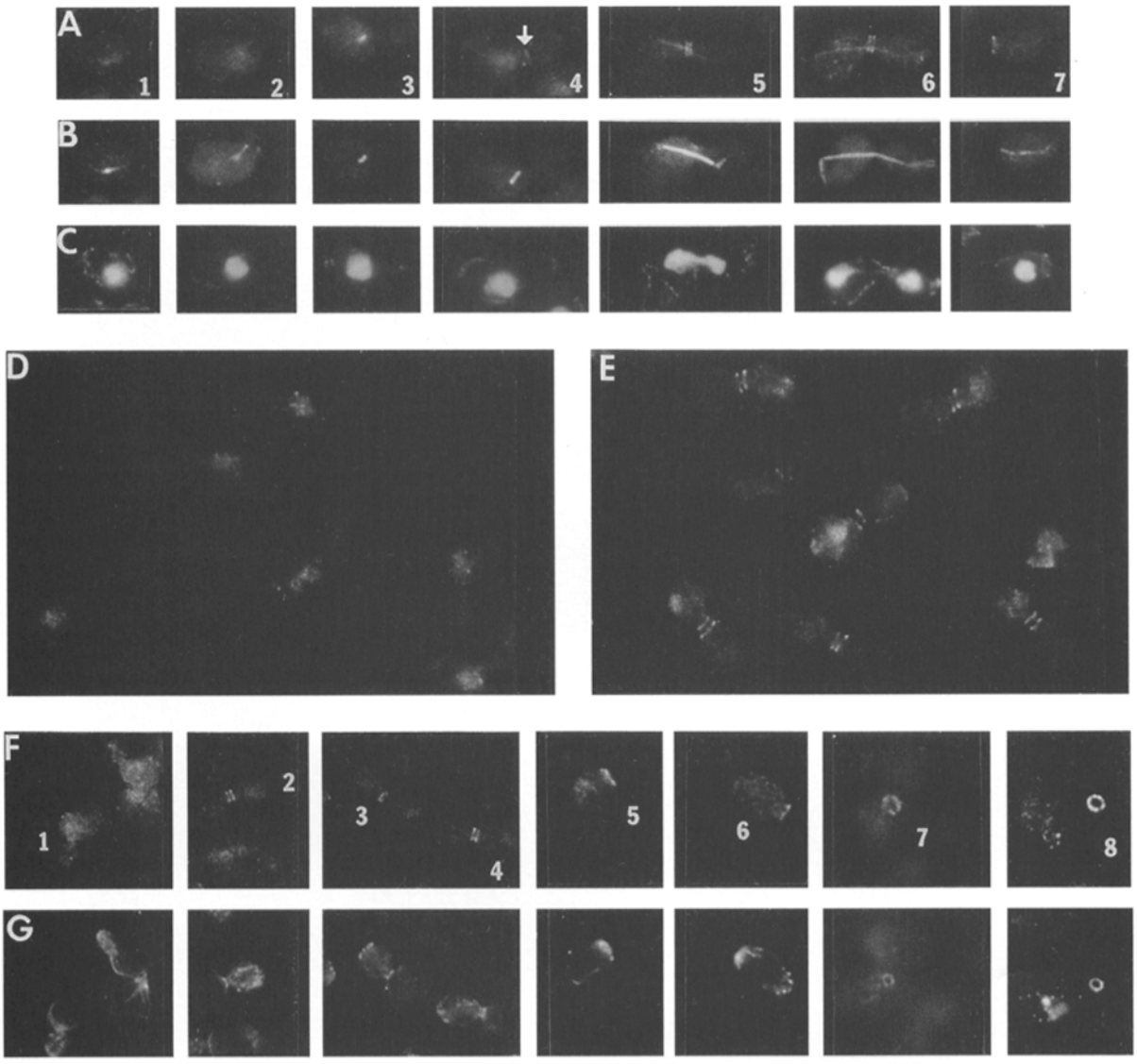

Figure 6. Timing of Bud3p assembly in relation to other cell-cycle markers. (*A–C*) Exponentially growing cells of wild-type α/α strain CP1AB-1BB were triple stained for Bud3p (*A*), tubulin (*B*), and DNA (*C*). Cells at progressively later stages of the cell cycle are shown from left to right; cell *7* is postcytokinesis. The arrow indicates the weak Bud3p staining at the neck of cell *4*. (*D* and *E*) Cells of strains CP1AB-1BB were arrested for 2 h with hydroxyurea (*D*) or nocodazole (*E*) and then stained for Bud3p. (*F* and *G*) Exponentially growing cells of strain C276 were double stained for Bud3p (*F*) and actin (*G*).

duplicated spindle pole bodies, but without an assembled spindle [Jacobs et al., 1988]). In cells arrested for 1.5–2 h with hydroxyurea, Bud3p was not detectable at the mother-bud neck (Fig. 6 *D*). In contrast, double rings of Bud3p were prominent in the necks of cells arrested with nocodazole (Fig. 6 *E*). Thus, it appears that Bud3p assembly at the neck requires the completion of DNA replication but not spindle assembly.

To correlate the assembly of Bud3p with the progressive reorganization of the actin cytoskeleton during the cell cycle (Kilmartin and Adams, 1984; Adams and Pringle, 1984; Lew and Reed, 1993), double-label experiments were performed using Bud3p-specific antibodies and rhodamine phalloidin. During the early stages of bud growth, the actin cytoskeleton is polarized towards the tip of the bud, and Bud3p is not detectable at the neck (Fig. 6, *F–G*, cell *1*). Subsequently, this tip orientation is lost (perhaps dependent upon the G2/M transition; Lew and Reed, 1993), and eventually actin reorients towards the mother-bud neck (perhaps dependent upon the metaphase-anaphase transition; Lew and Reed, 1993). As expected from the data already presented, the double-label experiments showed that Bud3p can assemble at the mother-bud neck well before actin fully reorients towards that site (Fig. 6, *F–G*, cell *2*). All cells in which actin had reoriented to the mother-bud neck also had Bud3p assembled there (Fig. 6, *F–G*, cells *3* and *4*).

To examine more closely the timing of Bud3p disassembly during the unbudded phase, we scored the presence or absence of a Bud3p ring in unbudded cells. On average, 80% of such cells (strain CP1AB-1BB, 79%, $n = 115$; strain C276, 80%, $n = 208$) had a single ring of Bud3p, indicating that Bud3p localization persists through most of the unbudded phase. We also compared Bud3p and actin organization to determine whether the Bud3p ring persists until the next round of polarity establishment before budding. Immediately after cell division, actin-containing structures persist at the preceding division site in unbudded cells. At approximately the time of Start (G1 Cdc28p kinase activation; Reed, 1992), actin-containing structures assemble at the future bud site (Kilmartin and Adams, 1984; Adams and Pringle, 1984; Ford and Pringle, 1991; Lew and Reed, 1993). Disassembly of the old and assembly of the new actin structures appear to occur independently, as unbudded cells can be observed with either, both, or neither structure (Ford and Pringle, 1991). In both α/α and **a**/α strains, most unbudded cells that exhibited Bud3p rings also exhibited actin concentrated in the same region (Fig. 6, *F–G*, cells *5–8*). In some cells, the actin appeared as a cluster of cortical patches (Fig. 6, *F–G*, cells *5* and *6*); in other cells, the actin appeared as a ring concentric with, and smaller in diameter than, the ring of Bud3p (Fig. 6, *F–G*, cells *7* and *8*). A small number of unbudded cells with Bud3p rings exhibited no corresponding concentration of actin (data not shown), indicating that the ring of Bud3p can persist at the division site beyond the time of actin disassembly at that site.

It is difficult to distinguish a new from an old actin concentration in α/α cells because, in cells that exhibit the axial-budding pattern, the new actin concentration forms adjacent to the concentration remaining at the previous division site. For this reason, bipolar-budding **a**/α cells were examined to determine whether the ring of Bud3p can persist beyond the time at which a new polarity axis assembles. As illustrated in Fig. 6, *F–G* (cell *6*), many unbudded cells (21/107 cells examined) were found in which the ring of Bud3p remained until a new concentration of actin had assembled at a distal site. In some of these cells (5/21), actin at the previous division site had disassembled, whereas in others (16/21) it remained, producing a cell with actin concentrations at both ends (Fig. 6, *F–G*, cell *6*). Thus, rings of Bud3p often persist until the new bud site begins to assemble in **a**/α cells and presumably also in α/α cells, given that the rings of Bud3p persist for the same proportion of the unbudded phase in such cells (see above).

Dependence of Bud3p Assembly upon the Neck Filament-associated Proteins

The rings of Bud3p observed on large-budded, dividing, and unbudded cells are indistinguishable from those observed with antibodies specific for the neck filament-associated proteins Cdc3p, Cdc10p, Cdc11p, and Cdc12p (Haarer and Pringle, 1987; Kim et al., 1991; Ford and Pringle, 1991; Kim, H., S. Ketcham, B. Haarer and J. R. Pringle, unpublished). However, in contrast to Bud3p, the neck filament-associated proteins assemble in a small ring on the cell surface ~15 min before bud emergence, and are then present at the mother-bud neck throughout the remainder of the cell cycle. The apparent colocalization of Bud3p and the neck filament-associated proteins during the later stages of the

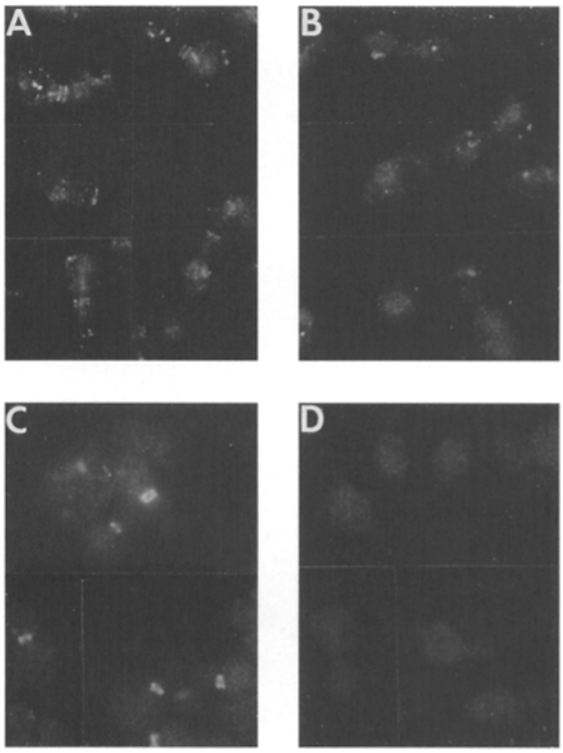

Figure 7. Dependence of Bud3p localization on *CDC12* function. An **a**/α *cdc12-6/cdc12-6* strain (JPTA1493-HO1) was grown at 23°C and then shifted to 37°C. The distributions of Bud3p (*A* and *B*) and Cdc3p (*C* and *D*) were examined by immunofluorescence during growth at 23°C (*A* and *C*) or 10 min after the shift to 37°C (*B* and *D*).

cell cycle suggests that Bud3p might assemble upon the neck filaments or associated proteins. To test this hypothesis, we used a temperature-sensitive *cdc12* mutant in which the neck filaments (as viewed by transmission electron microscopy: Adams, 1984) and associated proteins (as viewed by indirect immunofluorescence: Haarer and Pringle, 1987; Ford and Pringle, 1991; Kim et al., 1991) disassemble rapidly after shift from permissive (23°C) to restrictive (37°C) temperature. During growth at 23°C, rings of both Bud3p (Fig. 7 *A*) and Cdc3p (Fig. 7 *C*) were seen. However, neither structure could be detected in cells fixed 10, 20, 40, or 60 min after a shift to 37°C (Fig. 7, *B* and *D*). In a wild-type control strain (C276), rings of both Cdc3p and Bud3p were readily detectable after a comparable temperature shift (data not shown). These data suggest that both assembly and maintenance of the Bud3p rings are dependent upon the neck filaments and/or associated proteins.

To ask genetically whether the neck filaments are required for axial budding, the budding patterns of a *cdc11-6* strain were observed at 23°C and 37°C. (The *cdc12-6* mutant described above has a partial defect in the axial budding pattern even at permissive temperature.) At 23°C, the *cdc11-6* cells displayed typical axial budding as observed either by growth on agar (Fig. 8 *A*) or by staining of bud scars (Fig. 8 *C*). At 37°C, the mutant cells no longer budded consistently in the axial pattern (Fig. 8, *B* and *D*). Although there are the caveats that the buds formed by *cdc11* cells at 37°C are clearly abnormal and that the *cdc11* mutation is pleiotropic, these data are consistent with the hypothesis that the neck filaments and associated proteins have an essential role in axial budding. In contrast to these results, mutants defective in the *MYO1* gene (encoding a type II myosin), which also appear to have a cytokinesis defect (Watts et al., 1987; Rodriguez and Paterson, 1990), exhibit an axial pattern that is only slightly altered from that of wild-type cells (data not shown; see also Rodriguez and Paterson, 1990).

Discussion

Detailed analysis of the axial budding pattern (Chant and Pringle, 1995) has revealed that a daughter cell buds adjacent to its birth scar and a mother cell buds adjacent to its immediately preceding bud site. These observations suggest that the division site is marked in each cell cycle on both mother and daughter cells by a positional signal that can direct the selection of the new bud site. As only the immediately preceding division site strongly influences the selection of the new bud site (Chant and Pringle, 1995), and as the axial budding pattern is disrupted by temporary arrest of the cell cycle (Madden and Snyder, 1992; Chant and Pringle, 1995), the positional signal appears to be transient.

The immunolocalization data presented here show that the *BUD3* gene product behaves as predicted for the postulated positional signal for axial budding. Bud3p assembles in an apparent double ring at the mother-bud neck at about the time of mitotic spindle formation, remains for the duration of the cell cycle, and persists after division as a single ring marking the division site on both mother and daughter cells. The Bud3p signal is transient, as it disappears at about the time when the new polarity axis forms. The hypothesis that Bud3p is (or is part of) the positional signal for axial budding is supported by the genetic data. Both the original *bud3-1* mutation (Chant and Herskowitz, 1991) and the deletion mutations described here eliminate the axial budding pattern but have no detectable effect on the bipolar budding pattern.

An important question is whether Bud3p functions only in the generation of the axial budding pattern or has another role (e.g., in polarity establishment or cytokinesis). The observation that a complete deletion of *BUD3* produces no detectable abnormality other than the loss of axial budding supports the former hypothesis. However, it remains possible that Bud3p has another role that is masked by functional redundancy. This possibility gains some credibility from the observation that Bud3p is expressed and localized to the division site in a/α cells, where it has no detectable effect upon the budding pattern. A search for mutations that are synthetically lethal with the *bud3* deletion might shed light on this issue.

Three lines of evidence suggest that Bud3p assembles in the mother-bud neck by binding to the neck filaments or their associated proteins (see Introduction). First, the immunofluorescence localization of Bud3p in large-budded and unbudded cells is indistinguishable from that of the neck filament–associated proteins Cdc3p, Cdc10p, Cdc11p, and

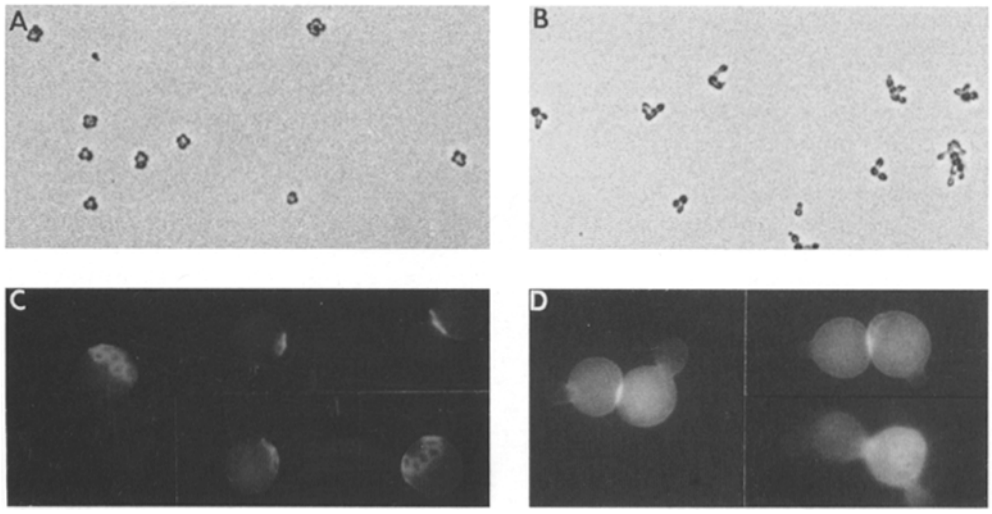

Figure 8. Alteration of the axial budding pattern produced by mutation of *CDC11*. An a *cdc11-6* strain (T515A) that had been grown exponentially overnight in liquid culture at 23°C was plated on agar medium at 23°C (*A*), or shifted to 37°C for 1 h, and then plated on agar medium at 37°C (*B*). In both cases, cells were then observed after 3 h of growth on agar. Cells from the same liquid culture were stained with Calcofluor during growth at 23°C (*C*) or 3 h after a shift to 37°C (*D*).

Cdc12p. Second, shift of a temperature-sensitive *cdc12* mutant from permissive to restrictive temperature results in a very rapid and apparently simultaneous loss of localization of both Bud3p and the neck filament–associated proteins. Third, mutations in the neck filament–associated proteins can cause a loss of axial budding (see also Flescher et al., 1993). The observation that a *myo1* mutation (Watts et al., 1987; Rodriguez and Paterson, 1990) has only a minor effect on the axial pattern indicates that not all mutants with defects in cytokinesis have strong defects in the axial pattern and thus supports the hypothesis that the neck filaments or their associated proteins have a direct role in producing the axial pattern. This interpretation expands our understanding of the functions of the neck filament–associated proteins, which had previously been implicated in the localization of chitin deposition, control of the pattern of cell-wall expansion during bud growth, and cytokinesis and septum formation. It appears that the neck filament–associated proteins may have a wide range of functions in the spatial organization of the cell surface (see also Neufeld and Rubin, 1994; Fares, J., M. Peifer, and J. R. Pringle, manuscript submitted for publication).

In contrast to Bud3p, the neck filament–associated proteins assemble at the presumptive bud site before bud emergence and are present in the mother-bud neck throughout the period of bud growth. Assembly of Bud3p at mid-cycle might reflect an abrupt rise in the level of Bud3p, a cell cycle-specific modification of Bud3p, or a modification of the neck filament template (by addition of a new protein or modification of one already present). It should be possible to investigate all of these possibilities with the reagents currently available, although an obstacle at present is our inability to detect Bud3p in blots of yeast proteins with the available antibodies. Whatever the precise mechanism, the onset of Bud3p assembly is probably triggered, directly or indirectly, by regulatory transitions in the cell cycle as controlled by the Cdc28p protein kinase and associated cyclins. The observations that Bud3p fails to assemble in hydroxyurea-arrested cells but does assemble in nocodazole-arrested cells suggest that assembly of Bud3p may require the completion of DNA synthesis and be triggered by one of the mitotic forms of the Cdc28p protein kinase (Weinert and Hartwell, 1993; Lew and Reed, 1993). Insight into this control should come from monitoring the status of Bud3p assembly in mutants that block at various points in the cell cycle.

It is also of interest to ask about the control of Bud3p disassembly late in the unbudded phase. This might be triggered specifically by activation of the Cdc28p protein kinase at Start (Reed, 1992). Alternatively, the gradual dissolution of the assemblies of neck filament–associated proteins after cytokinesis (Kim et al., 1991; Ford and Pringle, 1991; Kim, H., S. Ketcham, B. Haarer, and J. R. Pringle, unpublished), together with the dependence of Bud3p localization on these structures, may provide a sufficient explanation.

For axial budding to occur, Bud3p must communicate with downstream factors, namely the general bud-site selection proteins, the polarity establishment proteins, and ultimately the cytoskeleton. The sequence of Bud3p has as yet provided no clues as to how this communication might occur, but the immediate target of Bud3p is presumably the general bud-site selection proteins. These proteins comprise a GTPase cycle in which the Rsr1p(Bud1p) GTPase is controlled by the Bud2p GTPase-activating protein and the Bud5p guanine-nucleotide-exchange factor (Bender and Pringle, 1989; Chant et al., 1991; Powers et al., 1991; Ruggieri et al., 1992; Park et al., 1993; Bender, 1993); they presumably act to direct the action of the polarity establishment proteins. In particular, it appears that Rsr1p/Bud1p-GTP, but not Rsr1p/Bud1p-GDP, can interact with Cdc24p (Ruggieri et al., 1992), which in turn can direct the polarized assembly of the cytoskeleton (at least in part through its activation of another GTPase, Cdc42p; Zheng et al., 1994). Thus, if Bud3p can recruit or locally activate Bud5p, resulting in a local concentration of Rsr1p(Bud1p)-GTP, it would trigger a cascade of events resulting in cytoskeletal polarization, and eventually the formation of a bud, at an axial site. As the cytoskeletal polarization includes the formation of a new ring of neck filament–associated proteins, upon which Bud3p will assemble in the new cell cycle, Bud3p and the neck filament–associated proteins appear to be linked (by the general bud-site selection and polarity establishment proteins) into a cycle in which each provides the positional information for the assembly of the other (Fig. 9).

This model leaves open several interesting questions. For example, it is not understood how one particular point on the circumference of the Bud3p ring is chosen as the next bud site. We imagine that there is some form of cooperativity at some stage in the assembly of the bud site, which ensures that only one bud site assembles. As a single point on the cell surface is chosen for budding even in the absence of the general bud-site selection functions, when budding occurs at

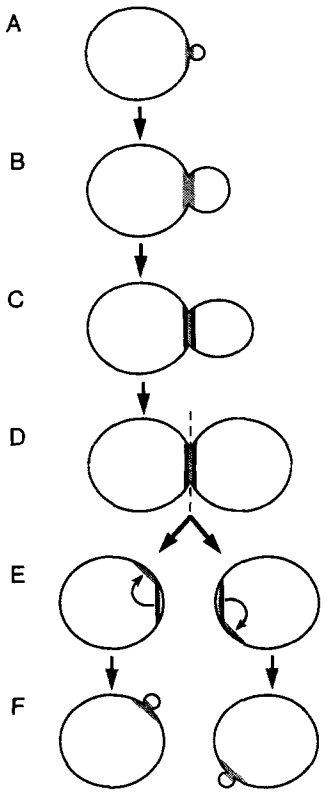

Figure 9. A cycle by which axial budding could be produced. The neck filaments and associated proteins (*light shading*) are assembled early in the cell cycle in a ring encircling the mother-bud neck (*A* and *B*). Later in the cell cycle, Bud3p (*dark shading*) assembles onto the neck filaments (*C*). At division, the Bud3p and neck-filament structures split (*D*), leaving superimposed rings of Bud3p and neck-filament proteins marking the division site on each progeny cell (*E*). As indicated by the arrows within the cells, the position of Bud3p then determines (via the general bud-site selection and polarity establishment proteins) the position of a new polarity axis adjacent to the previous division site (*E*). As part of the new polarity axis, a new ring of neck filaments and associated proteins forms, which will act as the template for Bud3p assembly in the new cell cycle. As the new buds form, the old rings of Bud3p and neck filament–associated proteins disassemble.

random locations, the mechanism that ensures the choice of a single bud site presumably operates through the polarity establishment functions.

In addition, it is not yet understood how the cell-type control of budding pattern is mediated. The expression and localization of Bud3p in **a**/α cells, where it has no detectable role in the budding pattern, indicates that a mechanism must exist such that the Bud3p rings are recognized by the general bud-site selection machinery in **a** and α cells but not in **a**/α cells. This mechanism is likely to involve some factor that is present in **a** and α cells but absent from **a**/α cells due to repression by the repressor **a1**-α2, as previously proposed (Chant and Herskowitz, 1991). Such a cell type–specific factor might modify Bud3p or coassemble with it. Candidates for this factor include the products of *BUD4* (Chant and Herskowitz, 1991) and of other axial-specific *BUD* genes, of which there are at least two (Chant, J., unpublished).

Finally, it may be asked whether the function of Bud3p in the axial budding pattern has parallels in other organisms. Because the mitotic spindle becomes aligned along the mother-bud axis and cleavage occurs perpendicular to this axis, the axial and bipolar patterns of bud-site selection give rise to two different patterns of cell division. Similar regulation of cell-division patterns is important to the morphogenesis of multicellular organisms. For example, the lack of cell migration in plants makes their morphogenesis particularly dependent upon intricate patterns of oriented cell divisions and directed cell growth (Gunning, 1982). It is plausible that sites of previous cell divisions might be used as marks to orient later cell divisions and that Bud3p-like molecules might be involved. Also striking is the similarity of the yeast cell division patterns to those of early *Caenorhabditis elegans* embryos (Hyman and White, 1987). Beginning at the two-cell stage, the AB blastomere and its progeny divide in a pattern in which each cleavage plane is perpendicular to the previous one (orthogonal pattern). In contrast, the P_1 blastomere and its progeny divide in a pattern in which successive cleavage planes are parallel (longitudinal pattern). The orthogonal division pattern, thought to be a default pattern, is due to the orientation of spindles arising from repeated centrosome duplication, separation, and spindle formation. In contrast, the longitudinal division pattern results from centrosome duplication, separation, and spindle formation followed by rotation of the spindle through 90°. Experimental evidence suggests that the spindles of P_1 cells are oriented by microtubules that are captured at the preceding site of cytokinesis and then rotate the spindle (Hyman, 1989). It will be interesting to see if the cytokinesis sites in the *C. elegans* blastomeres are marked by proteins like Bud3p.

We thank Michael Tibbetts for advice on the production of antibodies to Bud3p and members of the three laboratories for helpful discussions. We also thank Stephen Oliver for communicating unpublished data.

Grants from the National Institutes of Health support work in the laboratories of J. Chant (GM49782), I. Herskowitz (GM48052), and J. R. Pringle (GM31006). While in J. R. Pringle's laboratory, J. Chant was supported by a fellowship from the Damon Runyon-Walter Winchell Cancer Research Fund. While in I. Herskowitz's laboratory, J. Chant was supported by fellowships from the Medical Research Council of Canada, the Lucille P. Markey Charitable Trust, and the Weingart Foundation.

Received for publication 19 September 1994 and in revised form 19 January 1995.

References

Adams, A. E. M. Cellular morphogenesis in the yeast *Saccharomyces cerevisiae*. 1984. Ph.D. Thesis. University of Michigan, Ann Arbor, MI. pp. 179.

Adams, A. E. M., and J. R. Pringle. 1984. Relationship of actin and tubulin distribution to bud growth in wild-type and morphogenetic-mutant *Saccharomyces cerevisiae*. *J. Cell Biol.* 98:934–945.

Adams, A. E. M., and J. R. Pringle. 1991. Staining of actin with fluorochrome-conjugated phalloidin. *Methods Enzymol.* 194:729–731.

Bender, A. 1993. Genetic evidence for the roles of the bud-site-selection genes *BUD5* and *BUD2* in control of the Rsr1p (Bud1p) GTPase in yeast. *Proc. Natl. Acad. Sci. USA.* 90:9926-9929.

Bender, A., and J. R. Pringle. 1989. Multicopy suppression of the *cdc24* budding defect in yeast by *CDC42* and three newly identified genes including the *ras*-related gene *RSR1*. *Proc. Natl. Acad. Sci. USA.* 86:9976–9980.

Byers, B. 1981. Cytology of the yeast life cycle. *In* The Molecular Biology of the Yeast *Saccharomyces*: Life Cycle and Inheritance. J. N. Strathern, E. W. Jones, and J. R. Broach, editors. Cold Spring Harbor Laboratory, Cold Spring Harbor, New York. pp. 59–96.

Byers, B., and L. Goetsch. 1975. Behavior of spindles and spindle plaques in the cell cycle and conjugation of *Saccharomyces cerevisiae*. *J. Bacteriol.* 124:511–523.

Byers, B., and L. Goetsch. 1976. A highly ordered ring of membrane-associated filaments in budding yeast. *J. Cell Biol.* 69:717–721.

Chant, J., and I. Herskowitz. 1991. Genetic control of bud site selection in yeast by a set of gene products that constitute a morphogenetic pathway. *Cell.* 65:1203–1212.

Chant, J., and J. R. Pringle. 1991. Budding and cell polarity in *Saccharomyces cerevisiae*. *Curr. Opin. Genet. Div.* 1:342–350.

Chant, J., and J. R. Pringle. 1995. Patterns of bud-site selection in the yeast *Saccharomyces cerevisiae*. *J. Cell Biol.* 129:751–765.

Chant, J., K. Corrado, J. R. Pringle, and I. Herskowitz. 1991. Yeast *BUD5*, encoding a putative GDP-GTP exchange factor, is necessary for bud site selection and interacts with bud formation gene *BEM1*. *Cell.* 65:1213–1224.

Drubin, D. G. 1991. Development of cell polarity in budding yeast. *Cell.* 65:1093–1096.

Flescher, E. G., K. Madden, and M. Snyder. 1993. Components required for cytokinesis are important for bud site selection in yeast. *J. Cell Biol.* 122:373–386.

Ford, S. K., and J. R. Pringle. 1991. Cellular morphogenesis in the *Saccharomyces cerevisiae* cell cycle: localization of the *CDC11* gene product and the timing of events at the budding site. *Dev. Genet.* 12:281-292.

Freeman, G., and J. W. Lundelius. 1982. The developmental genetics of dextrality and sinistrality in the gastropod *Lymnaea peregra*. *Wilhelm Roux's Arch.* 191:69–83.

Gunning, B. E. S. 1982. The root of the water fern Azolla: cellular basis of development and multiple roles for cortical microtubules. *In* Developmental Order: Its Order and Regulation. P. B. Green, editor. Alan R. Liss, NY. 379–421.

Haarer, B. K., and J. R. Pringle. 1987. Immunofluorescence localization of the *Saccharomyces cerevisiae CDC12* gene product to the vicinity of the 10-nm filaments in the mother-bud neck. *Mol. Cell. Biol.* 7:3678–3687.

Hartwell, L. H. 1971. Genetic control of the cell division cycle in yeast. IV. Genes controlling bud emergence and cytokinesis. *Exp. Cell Res.* 69: 265–276.

Hyman, A. A. 1989. Centrosome movement in the early divisions of *Caenorhabditis elegans*: a cortical site determining centrosome position. *J. Cell Biol.* 109:1185–1193.

Hyman, A. A., and J. G. White. 1987. Determination of cell division axes in the early embryogenesis of *Caenorhabditis elegans*. *J. Cell Biol.* 105: 2123–2135.

Ito, H., Y. Fukuda, K. Murata, and A. Kimura. 1983. Transformation of intact yeast cells treated with alkali cations. *J. Bacteriol.* 153:163–168.

Jacobs, C. W., A. E. M. Adams, P. J. Szaniszlo, and J. R. Pringle. 1988. Functions of microtubules in the *Saccharomyces cerevisiae* cell cycle. *J. Cell Biol.* 107:1409–1426.

Kilmartin, J. V., and A. E. M. Adams. 1984. Structural rearrangements of tubulin and actin during the cell cycle of the yeast *Saccharomyces*. *J. Cell Biol.* 98:922–933.

Kim, H. B., B. K. Haarer, and J. R. Pringle. 1991. Cellular morphogenesis in the *Saccharomyces cerevisiae* cell cycle: localization of the *CDC3* gene product and the timing of events at the budding site. *J. Cell Biol.* 112: 535–544.

Kleid, D. G., D. Yansura, B. Small, D. Dowbenko, D. M. Moore, M. J. Grubman, P. D. McKercher, D. O. Morgan, B. H. Robertson, and H. L. Bachrach. 1981. Cloned viral protein vaccine for foot-and-mouth disease: responses in cattle and swine. *Science (Wash. DC).* 214:1125–1129.

Koerner, T. J., J. E. Hill, A. M. Myers, and A. Tzagoloff. 1991. High-expression vectors with multiple cloning sites for construction of *trpE* fusion genes: pATH vectors. *Methods Enzymol.* 194:477–490.

Lew, D. J., and S. I. Reed. 1993. Morphogenesis in the yeast cell cycle: regulation by Cdc28 and cyclins. *J. Cell Biol.* 120:1305–1320.

Lillie, S. H., and J. R. Pringle. 1980. Reserve carbohydrate metabolism in *Saccharomyces cerevisiae*: responses to nutrient limitation. *J. Bacteriol.* 143:

1384–1394.

Madden, K., and M. Snyder. 1992. Specification of sites for polarized growth in *Saccharomyces cerevisiae* and the influence of external factors on site selection. *Mol. Biol. Cell.* 3:1025–1035.

Meshcheryakov, V. N., and L. V. Beloussov. 1975. Asymmetric rotations of blastomeres in early cleavage of Gastropoda. *Wilhelm Roux's Arch.* 177: 192–203.

Messing, J. 1983. New M13 vectors for cloning. *Methods Enzymol.* 101:20–78.

Neufeld, T. P., and G. M. Rubin. 1994. The *peanut* gene of *Drosophila* is required for cytokinesis and encodes a protein similar to the putative bud neck filament proteins of *S. cerevisiae*. *Cell.* 77:371–379.

Oliver, S. G., Q. J. M. van der Aart, M. L. Agostoni-Carbone, et al. 1992. The complete DNA sequence of yeast chromosome III. *Nature (Lond.).* 357: 38–46.

Paquin, C., and J. Adams. 1982. Isolation of sets a, α, a/α, a/a and α/α isogenic strains in *Saccharomyces cerevisiae*. *Curr. Genet.* 6:21–24.

Park, H.-O., J. Chant, and I. Herskowitz. 1993. *BUD2* encodes a GTPase-activating protein for Bud1/Rsr1 necessary for proper bud-site selection in yeast. *Nature (Lond.).* 365:269–274.

Powers, S., E. Gonzales, T. Christensen, J. Cubert, and D. Broek. 1991. Functional cloning of *BUD5*, a *CDC25*-related gene from *S. cerevisiae* that can suppress a dominant-negative *RAS2* mutant. *Cell.* 65:1225–1231.

Pringle, J. R. 1991. Staining of bud scars and other cell wall chitin with Calcofluor. *Methods Enzymol.* 194:732–735.

Pringle, J. R., A. E. M. Adams, D. G. Drubin, and B. K. Haarer. 1991. Immunofluorescence methods for yeast. *Methods Enzymol.* 194:565–602.

Reed, S. I. 1992. The role of p34 kinases in the G1 to S-phase transition. *Annu. Rev. Cell Biol.* 8:529–561.

Rodriguez, J. R., and B. M. Paterson. 1990. Yeast myosin heavy chain mutant: maintenance of the cell type specific budding pattern and the normal deposition of chitin and cell wall components requires an intact myosin heavy chain gene. *Cell Motil. Cytoskeleton.* 17:301–308.

Rose, M. D., P. Novick, J. H. Thomas, D. Botstein, and G. R. Fink. 1987. A *Saccharomyces cerevisiae* genomic plasmid bank based on a centromere-containing shuttle vector. *Gene (Amst.).* 60:237–243.

Rose, M. D., F. Winston, and P. Hieter. 1990. Methods in Yeast Genetics. Cold Spring Harbor Laboratory Press, Cold Spring Harbor, NY. 123 pp.

Ruggieri, R., A. Bender, Y. Matsui, S. Powers, Y. Takai, J. R. Pringle, and K. Matsumoto. 1992. *RSR1*, a *ras*-like gene homologous to Krev-1 (*smg21A/rap1A*): role in the development of cell polarity and interactions with the Ras pathway in *Saccharomyces cerevisiae*. *Mol. Cell Biol.* 12: 758–766.

Rüther, U., and B. Müller-Hill. 1983. Easy identification of cDNA clones. *EMBO (Eur. Mol. Biol. Organ.) J.* 2:1791–1794.

Sambrook, J., E. F. Fritsch, and T. Maniatis. 1989. Molecular Cloning: A Laboratory Manual. Cold Spring Harbor Laboratory Press, Cold Spring Harbor, NY.

Sanger, F., S. Nicklen, and A. R. Coulson. 1977. DNA sequencing with chain-terminating inhibitors. *Proc. Natl. Acad. Sci. USA.* 74:5463–5467.

Singer, S. J., and A. Kupfer. 1986. The directed migration of eukaryotic cells. *Annu. Rev. Cell Biol.* 2:337–365.

Slater, M. L. 1973. Effect of reversible inhibition of deoxyribonucleic acid synthesis on the yeast cell cycle. *J. Bacteriol.* 113:263–270.

Snyder, M. 1989. The SPA2 protein of yeast localizes to sites of cell growth. *J. Cell Biol.* 108:1419–1429.

Snyder, M., S. Gehrung, and B. D. Page. 1991. Studies concerning the temporal and genetic control of cell polarity in *Saccharomyces cerevisiae*. *J. Cell Biol.* 114:515–532.

Sprague, G. F., Jr. 1991. Assay of yeast mating reaction. *Methods Enzymol.* 194:77–93.

Strome, S. 1993. Determination of cleavage planes. *Cell.* 72:3–6.

Tatchell, K., K. A. Nasmyth, B. D. Hall, C. A. Astell, and M. Smith. 1981. In vitro mutation analysis of the mating-type locus in yeast. *Cell.* 27:25–35.

Vallette, F., E. Mege, A. Reiss, and M. Adesnik. 1989. Construction of mutant and chimeric genes using the polymerase chain reaction. *Nucleic Acids Res.* 17:723–733.

Watts, F. Z., G. Shiels, and E. Orr. 1987. The yeast *MYO1* gene encoding a myosin-like protein required for cell division. *EMBO (Eur. Mol. Biol. Organ.) J.* 6:3499–3505.

Weinert, T. A., and L. H. Hartwell. 1993. Cell cycle arrest of *cdc* mutants and specificity of the *RAD9* checkpoint. *Genetics.* 134:63–80.

Wilkinson, L. E., and J. R. Pringle. 1974. Transient G1 arrest of *S. cerevisiae* cells of mating type α by a factor produced by cells of mating type a. *Exp. Cell Res.* 89:175–187.

Zheng, Y., R. Cerione, and A. Bender. 1994. Control of the yeast bud-site assembly GTPase Cdc42: catalysis of guanine nucleotide exchange by Cdc24 and stimulation of GTPase activity by Bem3. *J. Biol. Chem.* 269:2369–2372.

Ziman, M., D. Preuss, J. Mulholland, J. M. O'Brien, D. Botstein, and D. I. Johnson. 1993. Subcellular localization of Cdc42p, a *Saccharomyces cerevisiae* GTP-binding protein involved in the control of cell polarity. *Mol. Biol. Cell.* 4:1307–1316.